MATHEMATICAL CONTROL AND
RELATED FIELDS
Volume **2**, Number **2**, June **2012**

doi:10.3934/mcrf.2012.2.101

pp. **101–120**

NUMERICAL APPROXIMATION OF AN OPTIMIZATION PROBLEM TO REDUCE LEAKAGE IN WATER DISTRIBUTION SYSTEMS

Pierre Fabrie[1], Elodie Jaumouillé[2], Iraj Mortazavi[1]
and Olivier Piller[2]

1 Institut de Mathématiques de Bordeaux IMB UMR 5251
Institut Polytechnique de Bordeaux, Université de Bordeaux
F-33405 Talence, France
2 Irstea, UR REBX
F-33612 Cestas Cedex, France

(Communicated by Emmanuel Trélat)

Abstract. Leakage represents a large part of the supplied water in Water Distribution Systems (WDS). Consequently, it is important to develop some efficient strategies to manage such a phenomenon. In this paper an improved formulation of the hydraulic network equations that incorporate pressure-dependent leakage, is presented and validated. The formulation is derived from the Navier-Stokes equations and solved using an adequate splitting method. Then, this formulation is used to study a constrained optimization problem with the objective to minimize the distributed water volume reducing the leakage. The problem is described and validated for academic case studies and real networks.

1. **Introduction.** As leakage represents a large part of the water supplied in Water Distribution Systems (WDS), its decrease has considerable economical and environmental impact. Many studies related to leakage modeling in WDS have already been carried out where leakage level has been considered as a stochastic process [1] or a uniform parameter along a pipe (see [2] or Porteau [3], an object-oriented hydraulic modeling software developed by Irstea). Several parameters can be shown to impact leakage reduction. Specifically, pressure is one of the most significant factors influencing leakage in WDS [4, 5]. Therefore, it is important to take pressure-dependent leakage into account computing accurately advection-reaction-diffusion type Partial Differential Equations.

In this work, in order to predict more accurate hydraulic flows in WDS, an efficient computation of these PDE's corresponding to a physical model with a nonlinear operator related to the diffusion is proposed. This operator is known as the p-Laplacian and is used in some mathematical models associated with image processing, nonlinear diffusion, filtration, creeping flows in solids and quasi-Newtonian flows in general. Glowinski and Marrocco [6] have studied the finite element approximations of these models, using an implicit technique in order to solve the p-Laplacian equation.

2000 *Mathematics Subject Classification.* Primary: 76R99, 90C26.
Key words and phrases. Pressure-dependent leakage, splitting method, constrained optimization problem, pressure reduction.

Moreover, as the most significant factor influencing leakage is the pressure, it is important to act on the pressure to reduce leakage. To achieve this target, some constraints should be respected to better manage the pressure distribution: pressure must maintain sufficient values to satisfy consumers, but shouldn't be too large in order to avoid excessive leakage.

Then, a systematic leakage decrease procedure can be performed using a control operator in order to regulate pressure, minimizing the volume of leakage. This theory leads to the stabilization of the studied system and makes it more efficient, acting on a *control parameter*. This control is written as a constrained optimization problem with an objective function which depends on the control parameter (i.e. the pressure) to be minimized. The main term of this function is the distributed water volume. Minimizing the distributed volume of water is equivalent to minimizing the leakage volume. A gradient algorithm is used to solve this problem.

The new advances proposed in this paper consist of using the above numerical methods to solve a hydraulic stiff problem in WDS, taking into account that the leakage flow rate varies with the pressure nonlinearly. Furthermore, the minimization of the distributed water volume has an operational interest for the network administrator, because it minimizes directly the leakage volume. Usually, a pressure minimization at a point of the network is used. But the location of this point is difficult to find and can change with time due to hydraulic configurations. So the proposed method is more suitable to satisfy network administrator needs.

In the first part of this paper, the physical advection-reaction-diffusion model is presented. Then, a resolution of this model based on a splitting method is proposed and a Newton method of solving the p-Laplacian equation is detailed. In the second part, the leakage reduction problem is presented. A constrained optimization problem and the algorithm used to solve it, are then described. For both parts, model and methods are validated for academic and real networks.

2. **Pressure-dependent leakage model.**

2.1. **Physical model.**

An improved formulation of the hydraulic network equations which incorporates pressure-dependent leakage is presented in this section. This formulation is derived from the axisymmetric Navier-Stokes equations in cylindrical coordinates assuming incompressible fluid. It consists of an extension of the demand driven work [7]. The state variables are the flow rates and the heads in pipes [12].

2.1.1. *Governing equations.* The general hydraulic equation which represents flow rates in WDS is written as:

$$\frac{1}{gS}\frac{\partial Q}{\partial t}(t,x) + \frac{\partial H}{\partial x}(t,x) + \frac{1}{gS^2}\frac{\partial(\beta Q^2)}{\partial x}(t,x) + J(Q(t,x)) + \frac{\partial z}{\partial x}(x) = 0 \qquad (1)$$

with

$$J(Q(t,x)) = k|Q(t,x)|^{\gamma-1}Q(t,x) \qquad (2)$$

where Q denotes the flow rate or velocity flux on the cross-sectional area, H the piezometric head, g the gravitational acceleration, S the inside cross-sectional area of pipe, β the Boussinesq coefficient (constant in this paper), $J(Q)$ the head losses term, k the friction coefficient which depends on the units used, z the elevation

head from a data point to a point in the pipe and γ is an exponent which depends on the chosen formulation for head losses. The continuity equation reads:

$$\frac{\partial Q}{\partial x}(t,x) = -q_\ell \tag{3}$$

where q_ℓ denotes the leakage flow rate.

The leakage flow rate is often written in a general form:

$$q_\ell = c \max(0, H(t,x) - z(x))^\alpha \tag{4}$$

where c is a strictly positive leakage coefficient and α is a positive leakage exponent. As an example, the Torricelli equation is a particular case of the above equation for a leakage exponent equal to 0.5. To insure that the problem we deal with is well posed, the total head takes the form:

$$H = \frac{1}{c^{\frac{1}{\alpha}}}\left(\left|\frac{\partial Q}{\partial x}\right|\right)^{\frac{1}{\alpha}} + z \tag{5}$$

Assuming that $\dfrac{\partial Q}{\partial x} < 0$, that is the case in almost all situations, we obtain the following expression:

$$\frac{\partial}{\partial x}\left(\left|\frac{\partial Q}{\partial x}\right|^{\frac{1}{\alpha}}\right) = -\frac{\partial}{\partial x}\left(\left|\frac{\partial Q}{\partial x}\right|^{\frac{1}{\alpha}-1}\frac{\partial Q}{\partial x}\right) \qquad \text{whereas} \qquad \frac{\partial Q}{\partial x} < 0$$

Substituting $\dfrac{\partial H}{\partial x}$ by its expression related to Q in equation (5), the final governing flow rate equation (Eq. 1) reads:

$$\frac{1}{gS}\frac{\partial Q}{\partial t} - \frac{1}{c^{\frac{1}{\alpha}}}\frac{\partial}{\partial x}\left(\left|\frac{\partial Q}{\partial x}\right|^{\frac{1}{\alpha}-1}\frac{\partial Q}{\partial x}\right) + \frac{1}{gS^2}\frac{\partial(\beta Q^2)}{\partial x} + J(Q) + \frac{\partial z}{\partial x} = 0 \tag{6}$$

2.1.2. *Boundary conditions.* Here, it is convenient to introduce the definition of a connected graph to model WDS. The elements of a WDS are represented by nodes and edges. For sake of simplicity, an edge that is a collection of consecutive pipes will hereafter be referred to as a pipe. Boundary conditions depend on the type of nodes. In this paper, two boundary conditions are presented. Generally, for a tank taken as a node, the Neumann boundary condition - with the mass balance at the tank - is used. For the particular case of a tank with a unique connecting pipe, the boundary condition is:

$$\frac{\partial Q}{\partial x}(t) = -c\left\{H(t=0) - \int_0^t S_r^{-1} A^r Q(\tau) d\tau - z\right\}^\alpha \tag{7}$$

where S_r denotes the tank cross-sectional area and A^r is the incidence matrix reduced to tank nodes which contains 1 for outgoing pipes, -1 for incoming pipes and 0 otherwise.

For a non-tank node, boundary conditions depend on the number of connecting pipes. With a unique connecting pipe, the condition is the conservation of flow rate and the following Dirichlet condition is used:

$$Q(t) = d(t) \tag{8}$$

With several connecting pipes, another condition is necessary which represents the equality of heads on both sides of the node. Using the relation between head and

flow rate (Eq. 5), it is written as:

$$\left|\frac{\partial Q}{\partial x}\bigg|_{\Gamma_L}(t)\right| = \left|\frac{\partial Q}{\partial x}\bigg|_{\Gamma_R}(t)\right| \tag{9}$$

where Γ_L (resp. Γ_R) is the left (resp. the right) bound of the node.

2.2. **Numerical model.** The aim of this section is to present the numerical scheme we deal with, for simulating flow with pressure-dependent leakage in WDS. Two splitting methods are proposed to solve Eq. (6). The advantage of this approach is the use of a numerical solver fitted for each physical phenomenon.

2.2.1. *Splitting methods.* The advection-diffusion-reaction equation to solve is embedded in the more general form:

$$\frac{1}{gS}\frac{\partial Q}{\partial t} - \frac{1}{c^{\frac{1}{\alpha}}}\frac{\partial}{\partial x}\left(\left|\frac{\partial Q}{\partial x}\right|^{\frac{1}{\alpha}-1}\frac{\partial Q}{\partial x}\right) + \frac{\beta}{gS^2}\frac{\partial f(Q)}{\partial x} + J(Q) + \frac{\partial z}{\partial x} = 0, \tag{10}$$

with $f(Q) = Q^2$. The first idea is to solve this complete equation where advection, diffusion and reaction are coupled together. However, this technique requires using a fully implicit scheme or a semi-implicit one which suffers from strong stability restrictions [9].

Beale and Majda [8] have proved that it is important to separate advection and diffusion operators. Indeed, the numerical methods can be different to solve these two operators.

In this paper, we propose two methods to solve the physical advection-diffusion-reaction model. The first one consists of associating reaction with diffusion. In the second method, reaction is connected to advection. The order of convergence of such splitting techniques is in general one but it can be increased to 2 using a Strang splitting scheme (see for example Fabrie et al. [13]). However, in this paper considering the physical approximations and data uncertainties, the extension to Strang formulae is not implemented.

Splitting with advection and diffusion-reaction. The overall equation is split into two partial differential equations. The first represents the advection phenomenon as:

$$\frac{1}{gS}\frac{\partial Q}{\partial t} + \frac{\beta}{gS^2}\frac{\partial f(Q)}{\partial x} = 0 \tag{11}$$

The second represents the diffusion-reaction phenomenon:

$$\frac{1}{gS}\frac{\partial Q}{\partial t} - \frac{1}{c^{\frac{1}{\alpha}}}\frac{\partial}{\partial x}\left(\left|\frac{\partial Q}{\partial x}\right|^{\frac{1}{\alpha}-1}\frac{\partial Q}{\partial x}\right) + J(Q) + \frac{\partial z}{\partial x} = 0 \tag{12}$$

Splitting with advection-reaction and diffusion. The general equation is separated into two partial differential equations. The advection-reaction is written:

$$\frac{1}{gS}\frac{\partial Q}{\partial t} + \frac{\beta}{gS^2}\frac{\partial f(Q)}{\partial x} + J(Q) + \frac{\partial z}{\partial x} = 0 \tag{13}$$

Then, the second equation represents the diffusion phenomenon:

$$\frac{1}{gS}\frac{\partial Q}{\partial t} - \frac{1}{c^{\frac{1}{\alpha}}}\frac{\partial}{\partial x}\left(\left|\frac{\partial Q}{\partial x}\right|^{\frac{1}{\alpha}-1}\frac{\partial Q}{\partial x}\right) = 0 \tag{14}$$

2.2.2. *Numerical scheme.* ***Irregular mesh***. Each pipe has been separately discretized in order to have different flow rates depending on pressure along the pipe:

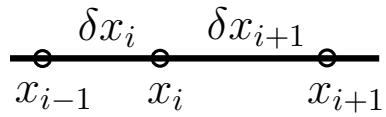

and let us note:

$$\delta x_i = x_i - x_{i-1} \quad \text{et} \quad \delta x_{i+1} = x_{i+1} - x_i$$

An irregular mesh is chosen in order to get accurate discretizations near junctions. For better readability, we will note: $Q_i = Q(x_i)$, $Q_{i+1} = Q(x_i + \delta x_{i+1})$ and $Q_{i-1} = Q(x_i - \delta x_i)$.

Splitting with advection and diffusion-reaction. The advection equation is solved using an explicit upstream finite-difference technique. This first-order scheme is written as:

$$\begin{aligned} Q_i^{n+\frac{1}{2}} = Q_i^n \quad &- \quad \frac{\beta \delta t}{S}\left\{\left(\frac{f(Q_i^n) - f(Q_{i-1}^n)}{Q_i^n - Q_{i-1}^n}\right)^+ \frac{Q_i^n - Q_{i-1}^n}{\delta x_i}\right\} \\ &+ \quad \frac{\beta \delta t}{S}\left\{\left(\frac{f(Q_{i+1}^n) - f(Q_i^n)}{Q_{i+1}^n - Q_i^n}\right)^- \frac{Q_{i+1}^n - Q_i^n}{\delta x_{i+1}}\right\} \end{aligned} \tag{15}$$

with

$$f(Q) = Q^2 \tag{16}$$

and

$$u = u^+ - u^- \quad \text{and} \quad |u| = u^+ + u^-$$

where δt is the time step, δx_i and δx_{i+1} the space steps.

In order to discretize the nonlinear diffusive term, the mesh around a point i is represented as:

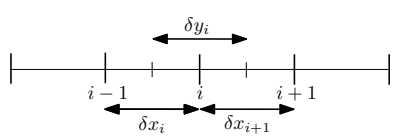

and the corresponding approximation reads:

$$\left(\frac{\partial F}{\partial x}\right)_i = \frac{F_{i+\frac{1}{2}} - F_{i-\frac{1}{2}}}{\delta y_i}$$

with $\delta y_i = \dfrac{\delta x_i + \delta x_{i+1}}{2}$, $\quad F_{i+\frac{1}{2}} = \dfrac{F_{i+1} - F_i}{\delta x_{i+1}} \quad$ et $\quad F_{i-\frac{1}{2}} = \dfrac{F_i - F_{i-1}}{\delta x_i}$

Finally, the diffusion-reaction equation at point i, is discretized as follows:

$$\begin{aligned} Q_i^{n+1} &= Q_i^{n+\frac{1}{2}} - gS\delta t\left\{ J(Q_i^{n+\frac{1}{2}}, Q_i^{n+1}) + \frac{\partial z}{\partial x} \right\} \\ &+ \frac{2gS\delta t}{c^{\frac{1}{\alpha}}(\delta x_i + \delta x_{i+1})}\left\{ \left| \frac{Q_{i+1}^{n+1} - Q_i^{n+1}}{\delta x_{i+1}} \right|^{\frac{1}{\alpha}-1} \frac{Q_{i+1}^{n+1} - Q_i^{n+1}}{\delta x_{i+1}} \right. \\ &- \left. \left| \frac{Q_i^{n+1} - Q_{i-1}^{n+1}}{\delta x_i} \right|^{\frac{1}{\alpha}-1} \frac{Q_i^{n+1} - Q_{i-1}^{n+1}}{\delta x_i} \right\} \end{aligned} \tag{17}$$

with

$$J(Q_i^{n+\frac{1}{2}}, Q_i^{n+1}) = k|Q_i^{n+\frac{1}{2}}|^{\gamma-1} Q_i^{n+1} \tag{18}$$

A Newton method is used to solve Eq. 17. This method allows results for the physical leakage exponent range to be obtained (i.e. $0.5 \leq \alpha \leq 2.5$). Otherwise a classic resolution - such as a linear system resolution - may not converge for a large leakage exponent because of the nonlinearity of diffusion terms (i.e. the third term on the righthand side of Eq. 17).

Splitting with advection-reaction and diffusion. The second splitting method that we propose associates the reaction term with the advection one. The semi-implicit scheme of the advection-reaction equation is written as:

$$\begin{aligned} Q_i^{n+1/2} &= \frac{1}{1 + gS\delta tk\,|Q_i^n|^{\gamma-1}}\left(Q_i^n - \frac{\beta\delta t}{S}\left[\left(\frac{f(Q_i^n) - f(Q_{i-1}^n)}{Q_i^n - Q_{i-1}^n} \right)^+ \frac{Q_i^n - Q_{i-1}^n}{\delta x_i} \right.\right. \\ &- \left.\left. \left(\frac{f(Q_{i+1}^n) - f(Q_i^n)}{Q_{i+1}^n - Q_i^n} \right)^- \frac{Q_{i+1}^n - Q_i^n}{\delta x_{i+1}} \right] - gS\delta t\frac{\partial z}{\partial x} \right) \end{aligned} \tag{19}$$

The full implicit scheme for the diffusion equation is generally:

$$\begin{aligned} Q_i^{n+1} = Q_i^{n+1/2} + \frac{gS}{c^{\frac{1}{\alpha}}}\frac{2\delta t}{(\delta x_i + \delta x_{i+1})}\left(\left\{ \left| \frac{Q_{i+1}^{n+1} - Q_i^{n+1}}{\delta x_{i+1}} \right|^{\frac{1}{\alpha}-1} \frac{Q_{i+1}^{n+1} - Q_i^{n+1}}{\delta x_{i+1}} \right\} \right. \\ \left. - \left\{ \left| \frac{Q_i^{n+1} - Q_{i-1}^{n+1}}{\delta x_i} \right|^{\frac{1}{\alpha}-1} \frac{Q_i^{n+1} - Q_{i-1}^{n+1}}{\delta x_i} \right\} \right) \end{aligned}$$

Stability condition. The CFL condition is determined from the advection equation which is solved with an explicit scheme. It is written as:

$$2\beta\frac{\delta t}{\delta x}\frac{\max_i |Q_i^n|}{S} \leq 1$$

where $\delta x = \min(\delta x_i, \delta x_{i+1})$.
This condition means that the numerical scheme should take into account all the physical time and space phenomena.

Splitting choice. The two splitting methods presented in this paper are tested on a model benchmark network. Similar results are obtained in term of loss of water volume, nevertheless the convergence rate is faster for the first splitting (i.e. advection and diffusion-reaction). Moreover, the resolution approaches for diffusive and reactive terms are implicit and semi-implicit, contrary to the advection that is solved using an explicit technique. Also, the reaction is a second order term

that can be more easily correlated to the diffusion ([8]). Therefore, the splitting algorithm with coupled diffusion and reaction terms is chosen to approximate this advection-diffusion-reaction model.

2.3. **Numerical convergence.** Using the splitting methods, it is important to be careful about their accuracy because their convergence is not automatic, in particular with boundary conditions. The poor convergence results of the splitting methods for advection reaction problems have been already shown by Hundsdorfer & Willen [14]. In this paper, as explained above, in order to have a flexible splitting behavior the diffusion and reaction terms are coupled for the approximation and the stability condition is also satisfied. Finally, it is useful to verify the numerical convergence with time, comparing the results for a simple pipe benchmark with different time steps. Here we choose a pipe with a tank (named *Res*) and five nodes (see figure 1):

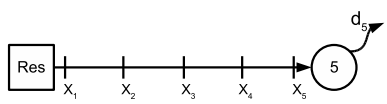

FIGURE 1. A simple pipe benchmark with a tank and five nodes.

To study the numerical convergence for the time discretization with a constant grid size, different time steps are used to measure the flow rate for the above mentioned pipe at different cross sections. In figure 2 the time step is varied from $\delta t = 15s$ until $\delta t = 100s$. As the figure shows there is a very small difference between different flow rates as the gap between the flow rate for $\delta t = 15s$ and $\delta t = 100s$ is only 0.04%. The effect of the time step choice on flow rates for nodes 2 and 3 is shown in figure 3. As the figure shows, the numerical convergence is again achieved with a difference of only 0.02%. Therefore, the choice of $\delta t = 100s$ for the paper's studies seems reasonable as the errors are every small and the numerical convergence is achieved for this time step.

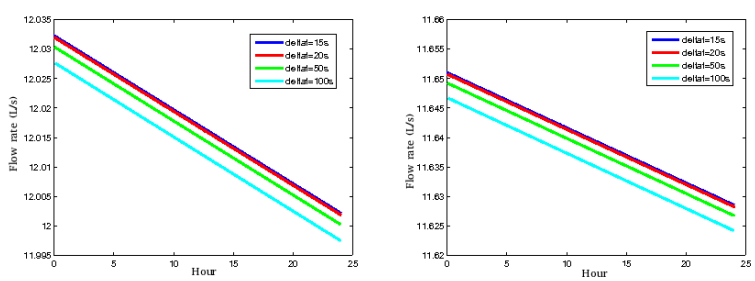

FIGURE 2. The flow rate of the tank (left) and the point 1 (right) for different time steps with constant space discretization.

2.4. **Results: Uncontrolled network properties.** Two networks (Fig. 4) are used to study the proposed pressure-dependent leakage model. These networks have been chosen because they contain several hydraulic characteristics that can be found

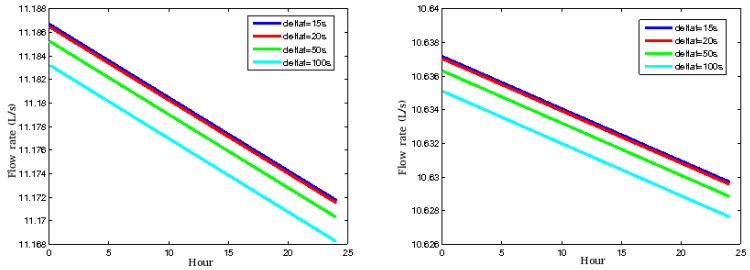

FIGURE 3. The flow rate of points 2 (left) and 3 (right) for different time steps with constant space discretization.

in real WDS. Thus, studying these test cases is a useful approach for real network modeling.

Network 1 is chosen to validate hydraulic properties by means of the transit between the two tanks. Network 2 is a simplification of Network 1 with only one tank. Consequently there is no transit between any tank. So, leakage influence on hydraulic parameters can be better observed since flow rates represent essentially consumption and leakage.

These networks contain six nodes and six pipes with a length of $1000\,m$, a diameter of $125\,mm$ and a friction coefficient of $k = 3.42\,10^{-5}$. Fifteen points are introduced along each pipe, generating between two locations a distance of $82.5\,m$ ($\delta x = 82.5$), except at the two extremities which is equal to $5\,m$. The computations are performed over a period of 24 hours with a time step of $100\,s$ ($\delta t = 100$).

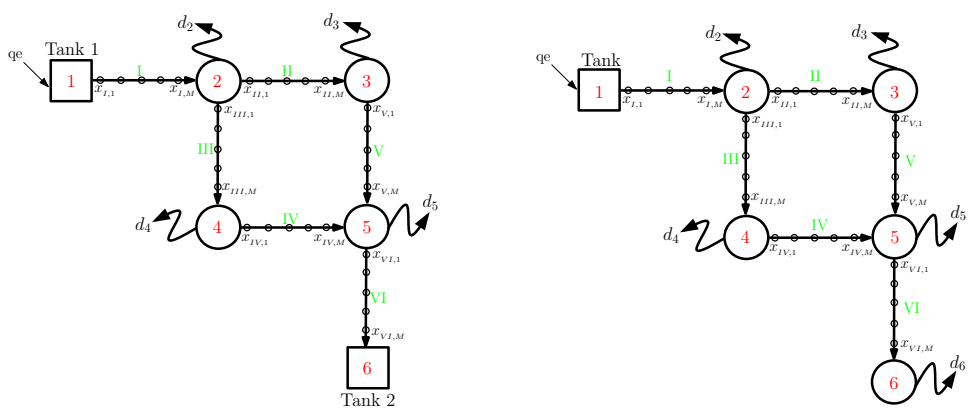

(a) Network 1 (b) Network 2

FIGURE 4. Benchmark pipe networks

Elevation heads associated to the six nodes of networks are presented in Tab. 1. They decrease linearly along each pipe.

2.4.1. *Network 1.* This network (Fig. 4(a)) contains two tanks and four consumption nodes. Tank 1 is the main tank and is supplied by a constant flow rate qe, corresponding to the mean of consumption and leakage over a day. Tank 2 provides

Node	1	2	3	4	5	6
z (m)	100	95	85	70	85	80

TABLE 1. Elevation head at each node of network 1 and 2

the network with water during high consumption periods (i.e. between $6:30\,am$ to $1\,pm$ and $5:30\,pm$ to $7\,pm$). One level of leakage is studied corresponding to $\alpha = 1$ (the linear case), which is frequently used when no information is available on leakage - and a leakage coefficient $c = 6.10^{-5}\,L/s/m^2$.
Flow rates and heads are presented at four locations on two pipes. These locations correspond to $0\,m$, $335\,m$, $665\,m$ and $1000\,m$ from the top of a $1000\,m$ length pipe.

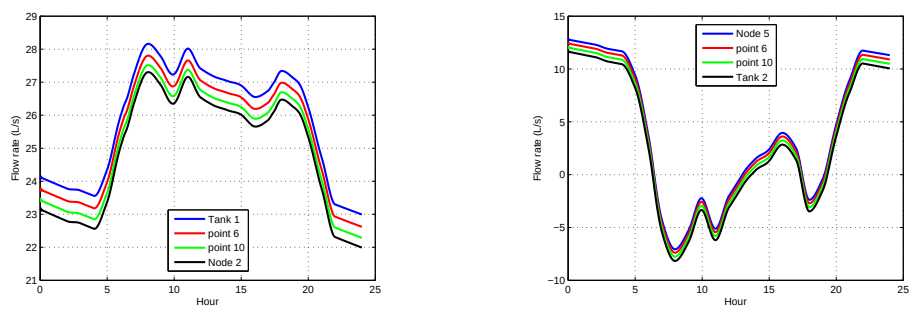

(a) Pipe I (b) Pipe VI

FIGURE 5. Flow rates along pipes I and VI on network 1

Due to the pressure-dependent leakage, the flow rate decreases along the pipe (e.g. from Tank 1 to node 2) (Fig. 5). The difference between two curves represents the leakage flow rate between two associated locations on the same pipe. The shape of flow rates on pipe I is uniform to that of consumption: large during peak consumption periods and smaller during low consumption periods. The sign of flow rates along pipe VI changes during a day (i.e at $6:30\,am$, $1\,pm$, $5:30\,pm$ and $7\,pm$) as the flow takes another path. During the low consumption periods, the flow goes from node 5 to Tank 2, and conversely during the high consumption periods.

The head at Tank 1 is almost constant because the flow rate qe is equal to the mean of consumption and leakage during the day. Thus, this tank is always in good working order at the end of the experiment. The head decreases along the pipe I because of the water friction on the wall.
The heads along pipe VI grows during the day according to the sign of flow rates. Indeed, Tank 2 supplies the network with water over peak consumption period (i.e. it becomes empty) and fills up during low consumption periods. Tank 2 is a balance tank: it provides assistance to the main tank in peak consumption periods.

The results for flow rates and heads obtained using this method are in good agreement with the values obtained using the Porteau software. Porteau does not take pressure-dependent leakage into account, nevertheless the order of magnitude of the results, for an equivalent flow rate as the above model, are the same as when imposing background leakage at nodes and intermediate points.

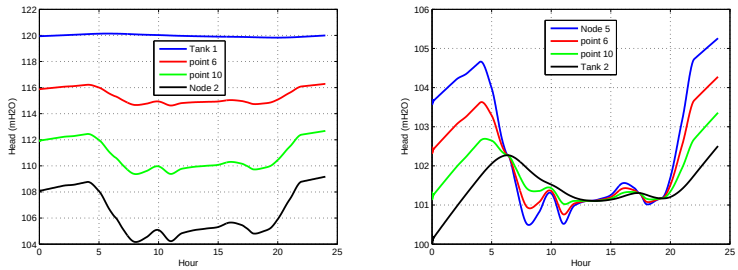

(a) Pipe I (b) Pipe VI

FIGURE 6. Heads along pipes I and VI on network 1

2.4.2. *Network 2.* In this example, the influence of leakage on flow rates and heads is studied. Network 2 (Fig. 4(b)) allows a better interpretation of results, because in this case there is no transit between tanks, and flow rates represent essentially consumption and leakage.
This network contains one tank, supplied with a constant flow rate qe, and five consumption nodes. Flow rates and heads along pipe V for different levels of leakage exponent (i.e. α =0.6, 1, 1.5, 2 and 2.2) are achieved. Results are shown for a coefficient $c = 6.10^{-6}\, L/s/m^{\alpha+1}$ calibrated for a leakage exponent equal to 1. Flow rates and heads are presented at the same four locations on pipes as the previous network.

The more the leakage exponents increase, the larger the difference between two locations along pipe is (Fig. 7). Because of the direct effect of the leakage exponent α to model flow rates, larger leakage exponents increase the flow rate in order to satisfy the consumption (Fig. 8(a)). Leakage can be assimilated to an additional consumption.
Higher leakage levels imply higher flow rates corresponding to smaller heads inside pipes. This behavior is observed in Fig. 8(b) noticing the magnitude of head curves for the different leakage exponents.

These results allow the presented pressure-dependent leakage model to be validated. Thus real networks can be more accurately modeled permitting better flow and pressure predictions. In the following, the governing equations serve as state equations for a leakage reduction problem at a daily scale.

3. **Control: Reducing the pressure to minimize the leakage.** The second part of this paper consists of the study of a control method to reduce leakage in WDS. As leakage represents a large part of the water supplied (with an order of magnitude of 30 %), its reduction is very important. This optimization scope is achieved forcing some pressure constraints. It is applied successfully to real networks.

3.1. **Optimization problem.** The choice of the control parameter, the objective function, constraints, boundary conditions and the algorithm are described in this section. Finally, this approach is validated for two networks. Here, a control point is assimilated to a control valve.

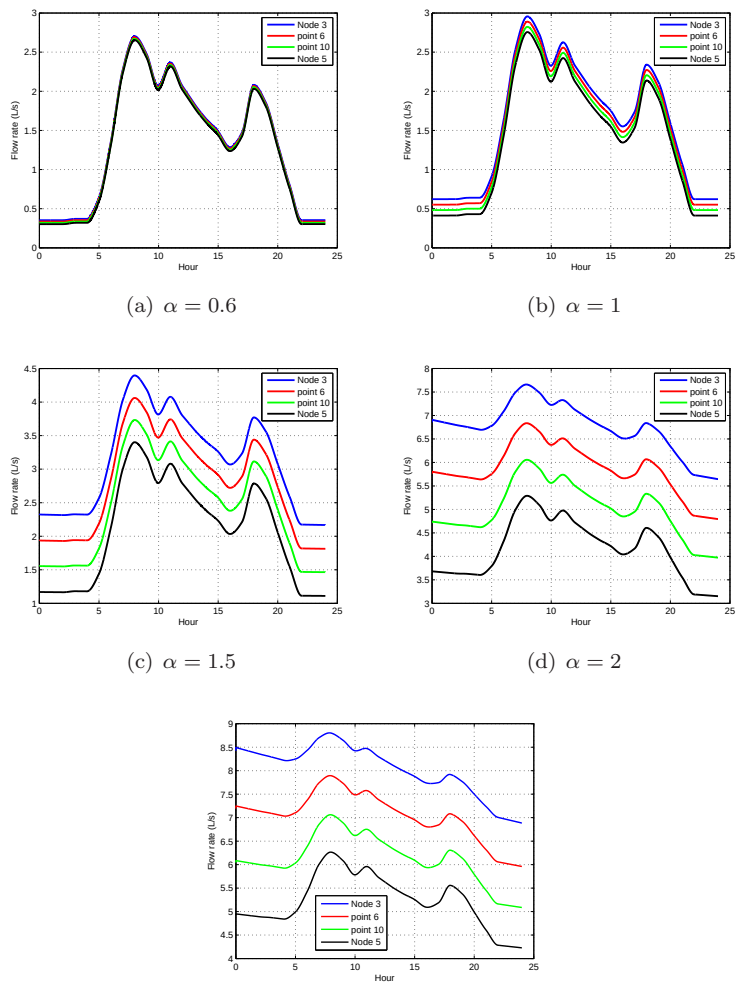

(a) $\alpha = 0.6$

(b) $\alpha = 1$

(c) $\alpha = 1.5$

(d) $\alpha = 2$

(e) $\alpha = 2.2$

FIGURE 7. Flow rates along pipe V on network 2 for different leakage exponents α

3.1.1. *Control parameter.* The control parameter is assimilated to a local head loss which is denoted by u. At the control point location, the value of u represents the pressure head reduction. The new pressure is written as $H_c - z = H - z - u$, where H_c is the controlled head and z is the ground level.

The admissible control set is defined as:

$$\mathcal{U}_{ad} = \{u \in L^2(0,T),\, u(t) \geq 0\}$$

with the following L^2 norm:

$$\|u\|_2 = \left(\int_0^T |u(t)|^2 dt \right)^{\frac{1}{2}}.$$

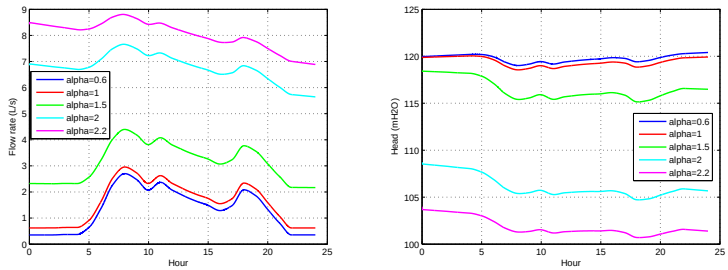

(a) Flow rates (b) Heads

FIGURE 8. Flow rates and heads at node 3 on network 2 for different leakage exponents α

The control parameter u can be zero: in this case no pressure reduction is possible. The larger the value of u, the more the control is effective.

3.1.2. *Objective function.* To combat water loss, many water utilities are developing methods to detect, locate, and correct leaks. This could be envisaged for important and detectable leaks. On the contrary, for background leakage, a good remediation is by pressure reduction. A water balance should be conducted. This is based on the measurement or estimation of water produced, imported, exported, consumed or lost. In this paper, we assumed that consumption and apparent losses (unauthorised consumption and metering inaccuracies) are not impacted by the control. In these conditions, minimizing the total volume of water distributed is equivalent to minimizing the real water losses or leakage volume.

Thus, the objective function can be written as ([10], [11]):

$$\begin{aligned} \mathcal{F}(u) &= \int_{t=0}^{T} \left\{ \|A^r Q(t,u)\|_2^2 + k_1 \|u(t) - u_{ref}(t)\|_2^2 \right\} dt \\ &+ k_2 \left\| A^r Q(T,u) - A^r Q_{ref} \right\|_2^2 \end{aligned} \tag{20}$$

where A^r is the incidence matrix reduced to tank nodes, u_{ref} is a given reference pressure which is time-dependent and depends on the control point number n_c (it can be written as $u_{ref}(t) = {}^t(u_{ref(1)}(t), \cdots, u_{ref(n_c)}(t))$, Q_{ref} is a given reference flow rate, and k_1 and k_2 are two positive constants. The first term represents the incoming water volume. The k_1 and k_2 coefficients are chosen to be very small to have a predominant term corresponding to the first term.

3.1.3. *Constraints and boundary conditions.* In order to get a realistic operational solution of the presented optimization problem, several hydraulic constraints are required.

Constraints. At a consumption node i, the controlled pressure must be sufficient to satisfy consumers demand. This constraint is written as:

$$H_c(t, x_i) - z(x_i) \geq H_{x_i,min} - z(x_i) \quad \forall t \in [0, T] \tag{21}$$

where $H_{x_i,min} - z(x_i)$ is the admissible minimal pressure. A tank i shouldn't be empty during the experiment in order to provide water to the network. So this constraint is written as:

$$H(t, x_i) - z_{bottom}(x_i) > 0 \quad \forall t \in [0, T] \tag{22}$$

where $z_{bottom}(x_i)$ is the height of the tank bottom.

Boundary conditions. The control parameter u appears in boundary conditions. If the control point is located at the tank outlet i, the boundary condition presented in the last part (Eq. 7) is rewritten as:

$$\frac{\partial Q}{\partial x}(t, x_i) = -c\left\{H(t = 0, x_i) - \int_0^t S_r^{-1} A^r Q(\tau) d\tau - z(x_i) - u(t)\right\}^{\alpha} \tag{23}$$

Thus the pressure at the tank outlet is reduced by the value of the parameter control.

If the control point is geometrically located after a consumption node, the boundary condition representing the head equality on both sides of this node (Eq. 9) is rewritten as:

$$\left|\frac{\partial Q}{\partial x}(t, x_{j,1})\right|^{\frac{1}{\alpha}} = \left|\frac{\partial Q}{\partial x}(t, x_{j-1,M})\right|^{\frac{1}{\alpha}} - c^{\frac{1}{\alpha}} u(t) \tag{24}$$

where $j - 1$ is the incoming pipe and j is the outgoing pipe. Thus, the pressure at the outlet of consumption node is reduced by the value of the control parameter u.

3.1.4. *Head computation.* At the control point location i, the head reads:

$$H(t, x_i) = \frac{1}{c^{1/\alpha}}\left(\left|\frac{\partial Q(t, x_i)}{\partial x}\right|^{1/\alpha}\right) + z(x_i) + u(t). \tag{25}$$

Moreover, the head is estimated using the equation (5) introduced previously in section 2.

3.1.5. *Direct resolution of the optimization problem.* In this section, the chosen control parameter approximation is explained and the algorithm used to solve the optimization problem is described.

Control parameter approximation. The control is assumed to be a step function given by:

$$u(t) = \sum_{i=1}^{N} u_i \varphi_i(t)$$

where φ_i is the base function defined by:

$$\varphi_i(t) = \begin{cases} 1 & \text{if } t \in [t_{i-1}, t_i[\\ 0 & \text{else} \end{cases}$$

The coefficients u_i are the unknowns which should be determined.

Algorithm. Here, the optimization problem is reduced to the computation of the u_i coefficients ($i = 1, \cdots, N$). A gradient algorithm is used to solve this problem and the gradient of the objective function is approximated by differential gradients. If a coefficient saturates a constraint, this constraint is kept saturated until the global convergence of the algorithm.

The developed algorithm is written as (for $u^k = {}^t(u_1^k, ..., u_N^k)$):

1. Initialization: $k = 0$: $u_1^0 = u_2^0 = ... = u_N^0 = 0$.
2. Iteration k: gradient method to calculate the u_i^{k+1}:

$$u^{k+1} = u^k - \rho_k \nabla \mathcal{F}(u^k) \tag{26}$$

where ρ_k is the descent step.

The derivative in the direction e_i of the function $\mathcal{F}$ is approximated by: $\frac{\mathcal{F}(u^k+he_i)-\mathcal{F}(u^k)}{h}$, for h small enough.
Therefore, the equation (26) becomes:

$$u^{k+1} = u^k - \rho_k \frac{\mathcal{F}(u^k + h) - \mathcal{F}(u^k)}{h}. \tag{27}$$

This is equivalent to computing:

$$\begin{cases} u_1^{k+1} = u_1^k - \rho_k \dfrac{\mathcal{F}(u_1^k + h, u_2^k, ..., u_N^k) - \mathcal{F}(u_1^k, u_2^k, ..., u_N^k)}{h} \\ u_2^{k+1} = u_2^k - \rho_k \dfrac{\mathcal{F}(u_1^k, u_2^k + h, ..., u_N^k) - \mathcal{F}(u_1^k, u_2^k, ..., u_N^k)}{h} \\ \vdots \\ u_N^{k+1} = u_N^k - \rho_k \dfrac{\mathcal{F}(u_1^k, u_2^k, ..., u_N^k + h) - \mathcal{F}(u_1^k, u_2^k, ..., u_N^k)}{h}. \end{cases}$$

3. The stop criterion for each u_i^{k+1} is:
   - if one of constraints (21) or (22) is not satisfied over the interval $[t_{i-1}, t_i[$, stop for the concerned u_i;
   - else: $k = k + 1$ and go back to the step 2.
4. Flow rates and heads are computed using the pressure-dependent leakage model for determined optimal coefficients u_i.

3.2. **Results: Controlled network properties.** Two networks are used to validate the proposed optimization method. Network 3 (Fig. 9(a)) is a simple one which allows the method to be validated and an understanding of how the leakage is influenced by pressure reduction. Then, network 4 (Fig. 14) - a real network - is used to prove the robustness of the method and to study the influence of the control point location on leakage reduction. This network is used to work with real data and is studied to bring to the fore the real economy on leakage. For this later network, fifteen points are introduced along each pipe with an identical irregular mesh as the one used in the first section.

3.2.1. *Network 3.* This network (Fig. 9(a)) contains one tank and one consumption node. It contains the main characteristics of networks and allows the understanding of control influences on hydraulic phenomena. The pipe has a 125 mm diameter and a friction coefficient k equal to $8.32\,10^{-5}$. The consumption value on the node 2 (Fig. 9(b)) is given. It changes during the day depending on low and high consumption times.
Different levels of leakage are studied corresponding to leakage exponents α equal to 0.5, 1 and 1.5, and a leakage coefficient c equal to 6.10^{-5}.
One control point is located at the tank's outlet and is represented with a cross on the first pipe. A control point is assimilated to a control valve.

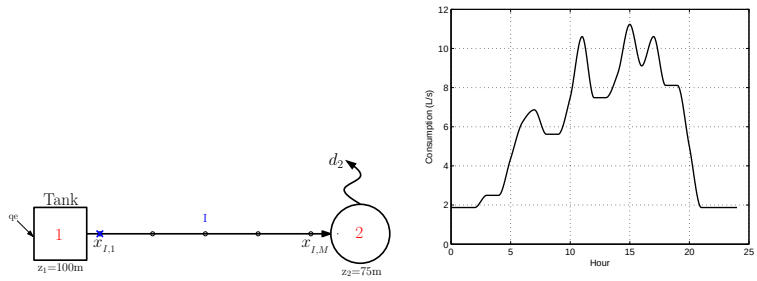

(a) Network 3 (b) Consumption at node 2

FIGURE 9. Network and consumption

A control function is sought which represents how much the pressure at the tank's outlet can be reduced. A first test consists of finding the number of steps in the control function. Two functions are presented in Fig. 10 for five and ten steps, and for a leakage exponent equal to 1. The shapes of these curves are similar. Nevertheless, the greater the number of steps, the more the shape of the control function and the inverse shape of consumption function are alike. For these two functions, results on leakage are identical (Tab. 2). For this example, a finer discretization is not necessary.

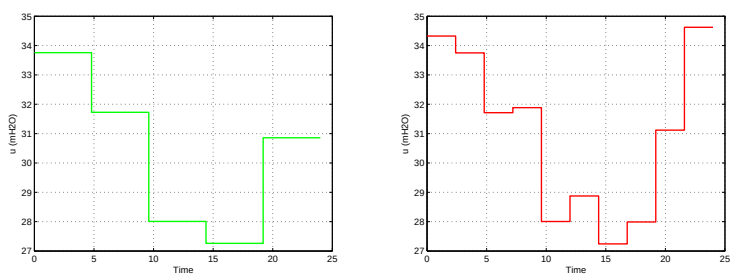

FIGURE 10. Control function for five and ten steps

	uncontrolled network	controlled network five steps function	controlled network ten steps function
Percent of leakage (%)	24.2	10.3	10.3

TABLE 2. Percent of leakage during a day on network 1 for different steps in control function with $\alpha = 1$

The control function obtained for different leakage and a five step function is presented in Fig. 11. The control is not constant which implies that the pressure can not be reduced identically during a day. During high consumption periods (i.e. steps 3 and 4), the control is smaller than during low consumption periods. Indeed to satisfy large consumptions, the control is smaller. Furthermore, the larger the leakage exponent, the less efficient the control is. In fact, pressure must be large

enough in order to satisfy consumption needs despite a large leakage and so small control. The level of leakage has no influence on the shape of the control function.

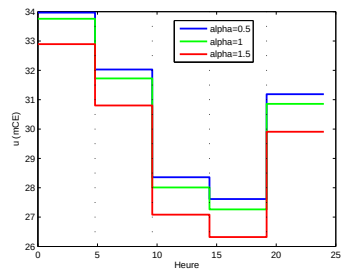

FIGURE 11. Control function

Uncontrolled and controlled flow rates at the tank's outlet are compared for different leakage exponents (Fig. 12). For all of them, the controlled flow rate is smaller. Indeed, the control problem is written to reduce the leakage which is equivalent to reducing the introduced water volume.

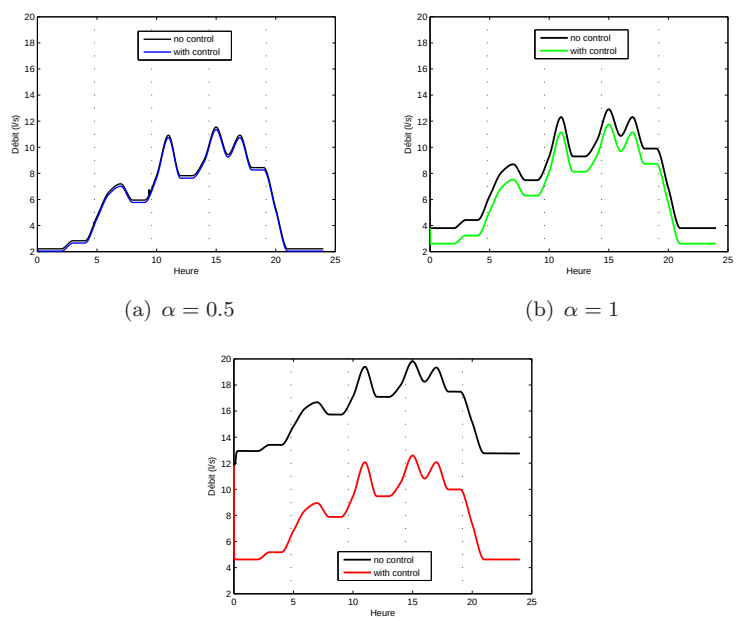

(a) $\alpha = 0.5$ (b) $\alpha = 1$

(c) $\alpha = 1.5$

FIGURE 12. Flow rates at the tank's outlet.

Uncontrolled and controlled heads at node 2 are compared for a leakage exponent equal to 0.5 (Fig. 13). The controlled head is smaller than the uncontrolled head. This is due to the definition of the controlled head H_c (i.e. $H_c = H - u$ with $u > 0$). In order to satisfy the pressure constraint (chosen equal to $10\,m$) at node 2,

the controlled head must be greater than $85\,m$ on each step. Indeed by definition $H_c(t, x_{I,M}) - z(x_{I,M}) > 10\,m$ with $z(x_{I,M}) = 75\,m$.
The constraint on the admissible controlled head is identical for different leakage exponents. On each step, the problem is constrained by the point with larger consumption.

For all exponents the leakage is reduced using the proposed control algorithm (Tab. 3). In fact, a pressure reduction induces a leakage reduction. To show the influence of leakage exponents on results, the leakage coefficient is held unvaried. This example is interesting to test the robustness of the method.

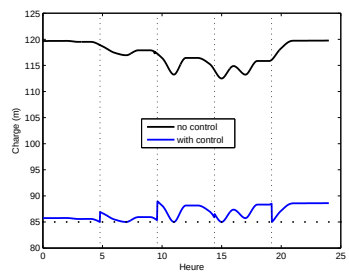

FIGURE 13. Heads at node 2 for $\alpha = 0.5$

	uncontrolled network	controlled network
$\alpha = 0.5$	5.4%	2.6%
$\alpha = 1$	24.2%	10.3%
$\alpha = 1.5$	63.4%	27.7%

TABLE 3. Rate of leakage during a day for the network 3

3.2.2. *Network 4: A real network.* In this section, a real network - a city from the southwest of France - is studied (Fig. 14). Thus the robustness of the proposed method is validated on the scale of a city and the influence of the suggested control problem on leakage is shown. This network is composed of 77 pipes and 63 nodes. The length, the diameter and the friction coefficient vary from one pipe to another. Two parts can be distinguished. Part 1 is a hilly zone where the elevation heads are high. Part 2 is a plane one where the elevation heads are low (i.e. near sea level). Part 1 contains two tanks and provides water to part 2. Winter season is observed during which consumptions are low and consequently the pressure is high. One leakage level is studied with a leakage exponent equal to 1 and a leakage coefficient $c = 2.10^{-6}\,L/s/m^2$.
In this example, the effect of a control point location on leakage is examined.

The first experiment is to place a control point at the main tank's outlet as it is indicated in figure 15. Thanks to this control n^o1, leakage is reduced: the leakage rate is decreased from 24.3 % to 22.3 % (Tab. 4). Nevertheless, the advantage is not as significant as we could expect. In fact, in order to satisfy all consumers, pressure can not be drastically reduced due to high elevation heads in part 1 (as part 1 is a hilly one).

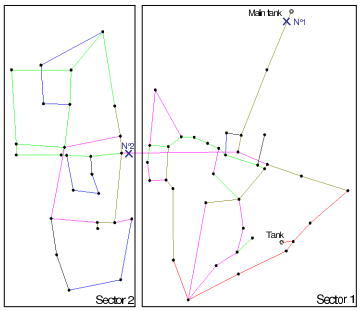

FIGURE 14. Network 4: A real network

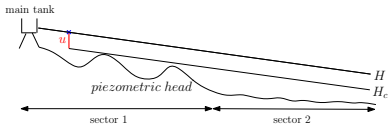

FIGURE 15. Control n^o1: control point at the tank's outlet

In order to optimize the leakage reduction, the control point is moved. It is located at the end of part 1 (i.e. after high piezometric heads zone). This control (n^o2) is more accurate because leakage represents 21.2 % of losses. During a day, this corresponds to a gain of the annual consumption of an inhabitant. In this case, part 1 is uncontrolled whereas part 2 is controlled efficiently (see figure 16 & table 4).

To optimize the problem, the two control points are simultaneously placed on the network. Thus, the control n^o1 reduces pressure in part 1 and the control n^o2 reduces pressure in part 2. The optimization of the problem is then more efficient. Leakage represents 19.1 % of the water supply, and the water volume gain by leakage reduction on a day is equivalent to the annual consumption of 1.7 inhabitants (see table 4).

Nevertheless to switch to several control points is very expensive. The choice between an optimal leakage reduction and an optimal cost of equipment has to be taken into account by the network administrator.

uncontrolled network	controlled sector 1	controlled sector 2	controlled sectors 1 et 2
24.3%	22.3%	21.2%	19.1%

TABLE 4. Rate of leakage during a day for the network 4

4. **Conclusion.** Water losses may constitute a large amount of the distributed total water volume throughout water distribution systems. In this paper, a new model method is proposed that intends to minimize the total water volume distributed through leakage reduction.

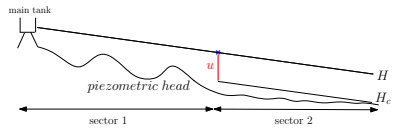

FIGURE 16. Control n^o2: control point at the end of the part 1

In the first part of this paper, governing equations of advection-reaction-diffusion type are derived from Navier-Stokes equations for incompressible flow and an explicit relationship between the local pressure and the leakage rate. The diffusive term is a p-laplacian operator. A two step splitting solution that separates advection from reaction/diffusion terms yields better results in terms of convergence rate. The advection equation is solved using an explicit upstream finite-difference scheme. The solution approaches for diffusive and reactive terms are implicit with Newton solving and semi-implicit. Results are presented and validated on two benchmark networks. This approach is original to solve this type of hydraulic problem. This technique allows pressure-dependent leakage to be taken into account, whereas in most models leakage is assumed to be uniform along a pipe.

In the second part, a constrained optimization problem is formulated for leakage reduction in WDS. The control variable has the mean of a local head loss and is considered in the Boundary Conditions to avoid dealing with discontinuities in the governing equations. The objective function to minimize is a regularization of the total water volume distributed. Specific operational constraints are added to ensure enough pressure at consumption points. The direct solution for this minimization problem is sought with a Gradient type method. The leakage reduction is proven to be significant in a case study. The percentage of leakage reduced from 24% to 10% in the linear relationship between pressure and leakage flow rate. With other leakage exponents, the same rate of reduction is achieved . The method was applied on a real network in the South-West of France. Controlling the pressure at two different strategic points permits a significant amount of the total distributed water to be saved (5%).

Future work will consist of applying a sensibility analysis of control location points to optimize the method.

REFERENCES

[1] O. Chesneau, "Un Outil d'aide à la Maîtrise des Pertes dans les Réseaux d'eau Potable: La Modélisation Dynamique de Différentes Composantes du Débit de Fuite," Ph.D thesis, University of Strasbourg, Strasbourg, 2006.

[2] E. Jaumouillé, O. Piller and J. E. Van Zyl, *A hydraulic model for water distribution systems incorporating both inertia and leakage*, in "CCWI2007 Water Management Challenges in Global Change," University of Exeter, UK, 129–135.

[3] Porteau software, IRSTEA (2011), accessed on March 09, 2012. Available from: http://porteau.irstea.fr/.

[4] A. Lambert, *What do we know about pressure-leakage relationships in distribution systems?*, in "Proc. of IWA Congress: System Approach to Leakage Control and Water Distribution Systems Management," Brno, Czech Republic, (2001), 89–96.

[5] J. E. Van Zyl and C. R. I. Clayton, *The effect of pressure on leakage in water distribution systems*, in "Proc. of CCWI Conference: Water Management for the 21st Century," University of Exeter, UK, **2** (2005), 131–136.

[6] R. Glowinski and A. Marrocco, *Sur l'approximation, par éléments finis d'ordre un, et la résolution, par pénalisation dualité, d'une classe de problèmes de Dirichlet non linéaires*,

Rev. Française Automat. Informat. Recherche Opérationnelle RAIRO Analyse Numérique, **9** (1975), 41–76.

[7] M. S. Ghidaoui, *On the fundamental equations of water hammer*, Urban Water Journal, **1 2**, 71–83.

[8] J. T. Beale and A. Majda, *Rates of convergence for viscous splitting of the Navier-Stokes equations*, Mathematics of Computation, **37** (1981), 243–259.

[9] S. Descombes and M. Massot, *Operator splitting for nonlinear reaction-diffusion systems with an entropic structure: Singular perturbation and order reduction*, Numerische Mathematik, **97** (2004), 667–698.

[10] E. Trélat, "Contrôle Optimal. Théorie & Applications," Mathématiques Concrètes, Vuibert, Paris, 2005.

[11] M. Bergounioux, "Optimisation et Contrôle des Systemes Linéaires," Dunod, 2001.

[12] B. Brémond, P. Fabrie, E. Jaumouillé, I. Mortazavi and O. Piller, *Numerical simulation of a hydraulic Saint-Venant type model with pressure-dependent leakage*, Applied Mathematics Letters, **22** (2009), 1694–1699.

[13] P. Fabrie, G. Gancel, I. Mortazavi and O. Piller, *Quality modelling of water distribution systems using sensitivity equations*, Journal of Hydraulic Engineering, **136** (2010), 11 pp.

[14] W. Hundsdorfer and J. G. Verwer, "Numerical Solution of Time Dependent Advection-Diffusion-Reaction Equations," Springer Series in Computational Mathematics, **33**, Springer-Verlag, Berlin, 2003.

Received April 2011; revised January 2012.

E-mail address: pierre.fabrie@math.u-bordeaux.fr
E-mail address: elodie.jaumouille@cerfacs.fr
E-mail address: Iraj.Mortazavi@math.u-bordeaux.fr
E-mail address: olivier.piller@irstea.fr